

The Stellar Parameters and Evolutionary State of the Primary in the d'-Symbiotic System StH α 190^{1,2}

Verne V. Smith

Department of Physics, University of Texas at El Paso, El Paso, TX 79968 USA

and

Claudio B. Pereira

Observatorio Nacional, Rua General José Cristino 77, CEP 20921-400, Rio de Janeiro BRAZIL

and

Katia Cunha

Observatorio Nacional, Rua General José Cristino 77, CEP 20921-400, Rio de Janeiro BRAZIL

Submitted to the Astrophysical Journal Letters

ABSTRACT

We report on a high-resolution spectroscopic stellar parameter and abundance analysis of a d' symbiotic star: the yellow component of StH α 190. This star has recently been discovered, and confirmed here, to be a rapidly rotating ($v \sin i = 100 \pm 10$ km s⁻¹) subgiant, or giant, that exhibits radial-velocity variations of probably at least 40 km s⁻¹, indicating the presence of a companion (as in many symbiotic systems, the companion is a hot white-dwarf star). An analysis of the red spectrum reveals the cool stellar component to have an effective temperature of $T_{\text{eff}} = 5300 \pm 150$ K and a surface gravity of $\log g = 3.0 \pm 0.5$ (this corresponds to an approximate spectral type of G4III/IV). These parameters result in an estimated primary luminosity of $45L_{\odot}$, implying a distance of about 780 pc (within a factor of 2). The iron and calcium abundances are found to be close to solar, however, barium is overabundant, relative to Fe and Ca, by about +0.5 dex. The Ba enhancement reflects mass-transfer of s-process enriched material when the current white dwarf was an asymptotic giant branch (AGB) star, of large physical dimension (≥ 1 AU). The past and future evolution of this binary system depends critically on its current orbital period, which is not yet known. Concerted and frequent radial-velocity measurements are needed to provide crucial physical constraints to this d' symbiotic system.

¹Based on observations made with the 2.1m telescope of McDonald Observatory, University of Texas, USA

²Based on observations made with the 1.52m telescope at the European Southern Observatory under the agreement with the Observatorio Nacional (Brazil)

Subject headings: binaries: individual (StH α 190)—binaries: symbiotic— stars: abundances—stars: rotation

1. INTRODUCTION

The object StH α 190 was discovered during an objective-prism survey for emission-line objects between -25° and 10° from the galactic plane by Stephenson (1986), who classified it as a symbiotic star. It is known that symbiotic stars are a class of interacting binary systems consisting of a cool, evolved star and a hotter companion star, with periods ranging from 1-3 years, up to 10-100 years (e.g. Allen 1982). Based on infrared colors, symbiotics can be divided into three groups: s-, d-, and d'-types (Webster & Allen 1975; Allen 1982). Those that show dust continuum emission between wavelengths of 1.0 and $5.0\mu\text{m}$ are classified as d-type and these systems contain a mass-losing Mira variable as a cool component. Those with a normal stellar spectrum in the infrared are classified as s-types. Typically, the shorter period symbiotics are found among the s-types while the longer period systems are found among the d-types. The possible binary properties of the d'-types are less known; for example, their binary periods (assuming they are binaries, as are the d- and s-types) are completely unknown. The d' stars also exhibit infrared dust emission, however, their dust color-temperatures are significantly lower than in the d-types. A more complete description about the known nature and properties of d'-types is given in Allen (1982) and Schmid & Nussbaumer (1993).

Schmid & Nussbaumer (1993) studied both optical and ultraviolet low-resolution spectra of StH α 190 and classified it as a d'-type symbiotic. More recently, Munari et al. (2001) have discovered that the cool component of StH α 190 is a rapidly rotating G-giant (with $v \sin i \sim 105 \text{ km s}^{-1}$). They also found that the system exhibits high-speed, bipolar mass outflow. In this *Letter* we report on an optical high-resolution spectroscopic analysis of StH α 190, with the principal goal being to derive basic parameters (effective temperature, surface gravity, chemical composition, evolutionary state, and radial velocity) of this symbiotic star.

2. OBSERVATIONS

The high-resolution spectra of StH α 190 analyzed here were obtained on two different telescopes. Four spectra were taken with the 2.1m telescope of McDonald Observatory with the Cassegrain cross-dispersed Sandiford echelle spectrometer plus CCD detector (McCarthy et al. 1993). In addition, five high-resolution spectra were obtained on the 1.52m telescope at the European Southern Observatory (ESO) with the fiber-fed coudé cross-dispersed echelle spectrometer FEROS and CCD detector (Kaufer et al. 1999). The McDonald spectra were taken at a two-pixel nominal resolving power of $R \approx 60,000$ and covering wavelengths from 6100\AA

to 7900Å, while the ESO FEROS spectrum has $R=48,000$, and with wavelength coverage from $\sim 4000\text{-}9000\text{\AA}$. A summary of all observations is shown in Table 1.

All McDonald spectra were reduced in a standard way with the IRAF software package. The echelle frames were background corrected and flat-fielded. The ESO spectra were reduced using the online pipeline reduction (Kaufer et al. 2000). Final S/N ratios were evaluated by the measurement of the rms flux fluctuations, with values ranging from $S/N=80\text{-}150$ in a continuum region at 6110Å. Spectra were checked for wavelength stability by using telluric O₂ lines near 6275Å as a reference and wavelength differences were less than 6mÅ ($\sim 0.3 \text{ km s}^{-1}$) from spectrum to spectrum.

3. ANALYSIS AND DISCUSSION

3.1. The Rotation of the Yellow Primary of StH α 190

Perhaps the most surprising aspect of StH α 190 is the presence of large numbers of absorption features broadened by a rather large rotational velocity (see also Munari et al. 2001). The wavelengths and strengths of many of these features coincide with absorption lines observed in late-F to early-K stars, e.g., Fe I or Ca I. For stars within this spectral range, high-resolution spectra can often be used to derive stellar parameters, as well as fairly detailed chemical compositions for a range of chemical elements. Due to the high rotational velocity of StH α 190, however, the obtainable spectral resolution is degraded, thus preventing an analysis based on measurements of individual equivalent widths. Instead, spectrum synthesis techniques must be used, as it is difficult to isolate features produced by only one species. Because of the difficulty in analyzing a range of different elements, in this *Letter* we concentrate on a small number of species (Fe I, Fe II, Ca I, and Ba II) to derive stellar parameters (T_{eff} and $\log g$) and rough chemical abundances in order to place constraints on the StH α 190 system. We confine a detailed analysis of selected absorption features to the red part of the spectrum for two reasons. First, the absorption line-density decreases considerably from blue to red, allowing for a clearer analysis of, as much as possible, nearly unblended spectral lines. Second, the possibility of light contamination (or veiling) from a hot companion, or hot gas in the system, diminishes towards the red. In particular, Schmid & Nussbaumer (1993) discussed light contamination of the cool component’s spectrum in StH α 190 and concluded that there was some contamination in the B-band, but very little by the V-band.

The rotationally broadened lines of StH α 190 can be seen in the two panels of Figure 1, where sample spectral regions from the ESO spectrum taken on Oct. 27, 1999 are displayed. The regions shown near 6150Å and 6430Å (as well as another region not illustrated near 5850Å) were selected to be synthesized because they contain a number of broadened features whose respective strengths are dominated approximately by single species, such as Fe I, Fe II, Ca I, and Ba II. Synthetic spectra covering the regions shown in Figure 1 (the smooth curves) were computed using a recent version of the LTE synthesis code MOOG (Snedden 1973), a Kurucz & Bell (1995) linelist with

solar g -values, and Kurucz ATLAS9 model atmospheres. The best-fit rotational velocity was determined by least-squares comparisons between observed and synthetic spectra. The top panel of Figure 2 shows values of χ^2 versus $v \sin i$. The lowest value found for χ^2 is used to normalize the larger values. It is clear from Figure 2 that there is a sharp minimum near $v \sin i = 100 \pm 10 \text{ km s}^{-1}$.

This fact can already be used to provide some constraints on stellar parameters if the assumption is made that the star is rotating at less than its critical breakup velocity, where

$$V_{\text{critical}} = \sqrt{\frac{GM}{R}} = [GMg]^{1/4}, \quad (1)$$

with M being the stellar mass, R its radius, and g its surface gravitational acceleration. The bottom panel of Figure 2 shows this critical velocity as a function of stellar mass for a series of surface gravities (shown as $\log g$), as well as the projected rotational velocity of StH α 190, shown as the dashed line with arrows at either end. The arrows indicate that this is a lower value for the rotational velocity of StH α 190, which could be considerably larger depending on the inclination angle. It is clear from the bottom panel of Figure 2 that, for any reasonable stellar mass, the surface gravity of StH α 190 must be larger than about $\log g \sim 1.5$, or the star would be rotating in excess of its critical velocity.

3.2. Stellar Parameters, Chemical Composition, & the Barium-Symbiotic Connection

The atmospheric parameters, effective temperature (T_{eff}) and surface gravity ($\log g$), along with $[\text{Fe}/\text{H}]$, $[\text{Ca}/\text{H}]$, and $[\text{Ba}/\text{H}]$ (where $[\text{X}/\text{H}] = \log(\text{N}(\text{X})/\text{N}(\text{H}))_{\star} - \log(\text{N}(\text{X})/\text{N}(\text{H}))_{\odot}$) abundances were determined using spectrum synthesis. The solution for T_{eff} and $\log g$ was obtained from a selection of 7 features near 6150Å, or 6430Å (and illustrated in Figure 1), as well as 5850Å, where a single species dominated so that they behaved almost as “single” spectral lines. Synthetic spectra covering a range in T_{eff} (from 4500 - 6500K), $\log g$ (from 2.0 to 4.0), and microturbulent velocity (from $\xi = 1.0$ to 3.0 km s^{-1}) were computed and then compared to the observed spectra. A least-squares comparison was used to select the best overall fits, with sample results illustrated for one particular set of models shown in the upper panel of Figure 3: results from a set of models with $\log g = 3.0$ and $\xi = 2.0 \text{ km s}^{-1}$ are presented for various effective temperatures. A set of models with fixed gravity and microturbulence is shown because the largest changes in the chemical abundances are found for changes in T_{eff} . Note that in this case, both Fe I and Fe II yield similar abundances for an effective temperature of 5300K. In all observed-synthetic comparisons over these parameter ranges, the Fe, Ca, and Ba abundances were allowed to vary in order to maximize the best fits.

Reinspection of Figure 1 shows that the Fe II features are quite sensitive to surface gravity. Estimates of the uncertainties in the derived stellar parameters would indicate that $\log g$ can be

constrained to about ± 0.5 dex, while T_{eff} is uncertain by about $\pm 150\text{K}$. We note that an earlier estimate of effective temperature for this star was given by Schmid & Nussbaumer (1992), based upon the dereddened (B-V), as $T_{\text{eff}} = 5150\text{K}$. The T_{eff} derived here would suggest a spectral type of about G4 (Schmid & Kaler 1982), compared to Munari et al.’s estimate of G7 and Mürset & Schmid’s estimate of G5. Based on the Schmid & Kaler calibration, the various estimated spectral types correspond to a range in T_{eff} from 5025–5300K.

It was found that the best overall fits can be obtained, based upon the Fe II features, with a gravity near $\log g = 3.0$ and $\xi = 2.0 \text{ km s}^{-1}$ (and these are the values used to construct the top panel of Figure 3). These fits also provide near-solar Fe and Ca abundances (Ca I is not plotted as it follows closely Fe I). Barium is an element produced primarily via s-process neutron-capture nucleosynthesis (e.g., Wallerstein et al. 1997). Note that in all models shown in the top panel of Figure 3, the Ba II 6141Å and 5853Å features provide [Ba/H] abundances considerably larger than [Fe/H] (or [Ca/H]). These results indicate that the G-type component in StH α 190 is enriched in Ba, relative to Fe, with [Ba/Fe] $\sim +0.5$. This enhancement in StH α 190 is most easily understood as resulting from mass transfer in the system when the white-dwarf member was a thermally-pulsing asymptotic giant branch (AGB) star, and was s-process enriched during its third dredge-up phase of stellar evolution. s-Process enhancements have been found in other symbiotic systems, such as AG Dra (Smith et al. 1996), He2-467 (Pereira et al. 1998), or S32 and UKS-Cel (Mürset & Schmid 1999).

With derived stellar parameters of $T_{\text{eff}} = 5300\text{K}$ and $\log g = 3.0$, the current primary of StH α 190 can be located in a $\log g - T_{\text{eff}}$ plane and compared to evolutionary tracks from stellar models. This comparison is shown in the bottom panel of Figure 3, with evolutionary tracks taken from Schaerer et al. (1993) and consisting of models computed with solar abundances. The parameters derived here suggest that the yellow component of StH α 190 consists of a star with $M \sim 2.5M_{\odot}$ nearing the base of the red giant branch. The values of mass, T_{eff} , and g can be used to estimate a luminosity of $L \sim 45L_{\odot}$ for the cool component of StH α , or $M_V \sim 0.65$. Adopting the V-magnitude from Munari et al. (2001) of $V = 10.5$ and $E(B-V) = 0.10$ (Schmid & Nussbaumer 1993), a distance of $\sim 780 \text{ pc}$ is derived. Uncertainties in the stellar mass, gravity, and T_{eff} lead to an uncertainty in this distance of about a factor of two ($d \sim 350\text{--}1500 \text{ pc}$). This distance is in fair agreement with Munari et al.’s estimate of 575 pc.

3.3. Radial Velocities and the Binary Nature of StH α 190

Radial velocities are also obtained from the comparisons of observed to synthetic spectra for StH α 190, which provided fairly accurate velocity estimates in spite of the line broadening. With nine spectra obtained over the time interval from 1995 to 2001, nine photospheric radial velocities are presented here for the G-star component in StH α 190. The heliocentric velocities are listed in Table 1 and cover a small range from 0 km s^{-1} to $+15 \text{ km s}^{-1}$. Munari et al. (2001) have also published radial velocities that overlap the values reported here and range over some 40 km s^{-1} in

amplitude. Both sets of radial velocities are on the same scale, as demonstrated by comparisons of interstellar Na D-line component velocities published by Munari et al. (2001) and those observed here (differences are, this study – Munari et al. = $-0.1 \pm 0.3 \text{ km s}^{-1}$). Taken together, the radial velocities indicate that StH α 190, like other symbiotics, is a binary, but almost certainly a closer binary than the d- and s-types. Munari et al. (2001) suggest a possible period for StH α 190 of 171 days, although such a period does not fit very well the radial velocities observed here. A possible shorter period of $\sim 37\text{--}39$ days may provide a better fit to both sets of radial velocities, however, more measured velocities, spanning time scales from a few days to a few weeks, will be needed to determine an accurate period.

A definitive orbital period is crucial in establishing the past, and future, history of StH α 190. Under the assumption that the primary is in synchronous rotation, a short orbital period would be required. In such a case, the projected rotational velocity of $v \sin i = 100 \text{ km s}^{-1}$ yields a maximum binary period of 4.2 days (derived from the mass estimate and gravity, which yields a radius of $8.3R_{\odot}$). Using the critical rotational velocity as an upper limit ($v \leq 230 \text{ km s}^{-1}$ from the bottom panel of Figure 2), then a lower limit to the binary period of 1.8 days is derived. In such a system, StH α 190 would have undergone common envelope evolution when the current white dwarf was an AGB star. The current evolutionary stage of the G-star suggests that it will soon ascend the red-giant branch, at which point another common envelope phase would occur, resulting in further orbital shrinkage. On the other hand, if the period is much longer ($\sim 1\text{--}6$ months) then the system has probably not undergone common envelope evolution and may not in the future. In this case, the rapid rotation of the G-star is probably due to spin-up from the accretion of material from a massive AGB wind (Jeffries & Stevens 1996).

With the few and scattered radial-velocity determinations to date, differences of at least 15 km s^{-1} , and probably as large as 40 km s^{-1} , are indicated. Observing StH α 190 intensively and obtaining high-quality spectra will allow for the determination of the orbital period, and will be crucial in establishing the past and future evolution of StH α 190.

4. CONCLUSIONS

The first high-resolution spectral analysis for stellar parameters and abundances in a d'-type symbiotic has revealed it to contain a rapidly rotating G-subgiant, or early giant, with $T_{\text{eff}} = 5300 \pm 150 \text{ K}$ and surface gravity of $\log g = 3.0 \pm 0.5$. Abundances of [Fe/H] and [Ca/H] indicate a near-solar metallicity, while barium is enhanced, with $[\text{Ba}/\text{Fe}] \sim +0.5$. Thus, StH α 190 is s-process enriched and probably accreted matter from its companion, now a white dwarf, when it was an s-process enriched thermally pulsing AGB star. Measured radial-velocity variations already betray the presence of the companion. If the rapid rotation of the cool component reflects synchronous rotation, then the current orbital period must be between about 1.8 to 4.2 days. If the orbital period is much longer than this, then the rapid rotation of the G-subgiant/giant is due presumably to the addition of angular momentum from a massive AGB wind (Jeffries & Stevens

1996). The current orbital period of StH α 190 is not yet well-constrained, so additional radial velocity measurements of this system, and other d'-symbiotics in general, are warranted.

We thank the staff of McDonald Observatory for technical support. This research is supported in part by the National Science Foundation (AST99-87374).

REFERENCES

- Allen, D. A. 1982, in *The Nature of Symbiotic Stars*. IAU Coll. No. 70 (Dordrecht: Reidel), eds. M. Friedjung & R. Viotti, p.27
- Jeffries, R. D., & Stevens, I. R. 1996, MNRAS, 279, 180
- Kaufer, A., Stahl, O., Tubbesing, S., Norregaard, P., Avila, G., François, P., Pasquini, L., Pizzella, A. 1999, Messenger, 95, 8
- Kaufer, A., Stahl, O., Tubbesing, S., Norregaard, P., Avila, G., François, P., Pasquini, L., Pizzella, A. 2000, in *Optical and IR Instrumentation and Detectors* Proc. SPIE, vol. 4008, eds. M. Iye, & A. F. Moorwood, p. 459
- Kurucz, R. L., & Bell, B. 1995, CD-ROM 23, Atomic Line Data (Cambridge: Smithsonian Astrophys. Obs.)
- McCarthy J. K., Sandiford B. A., Boyd, D. & Booth J. 1993, PASP, 105, 881
- Munari, U., et al. 2001, A&A, 369, L1
- Mürset, U., & Schmid, H. M. 1999, A&AS, 137, 473
- Pereira, C. B., Smith, V. V., & Cunha, K. 1998, AJ, 116, 1977
- Schaerer, D., Charbonnel, C., Meynet, G., Maeder, A., & Schaller, G. 1993, A&AS, 102, 339
- Schmid, H.M. & Nussbaumer, H. 1993, A&A, 268, 159
- Smith, V. V., Cunha, K., Jorissen, A., & Boffin, H. M. J. 1996, A&A, 315, 179
- Snedden, C. 1973, ApJ, 183, 839
- Stephenson, C. B. 1986, ApJ, 300, 779
- Wallerstein, G., et al. 1997, Rev.Mod.Phys., 69, 995
- Webster, B. L., & Allen, D. A. 1975, MNRAS, 171, 171

Fig. 1.— Two spectral regions in StH α 190 are shown, displaying the rotational profiles. Top panel: the observed StH α 190 spectrum is plotted along with three synthetic spectra (smooth curves) computed for three different surface gravities (at $T_{\text{eff}}= 5300\text{K}$), showing the sensitivity of the Fe II (and Ba II) to $\log g$. Bottom panel: the observed spectrum is shown as open circles. Three different synthetic spectra are shown to illustrate both the sensitivity of the Fe II to gravity, and the good agreement obtained between the 6140Å and 6430Å regions (which also agrees with analysis of a region near 5850Å).

Fig. 2.— Top panel: a least-squares comparison of observed - synthetic spectra for various values of $v \sin i$ to illustrate the derivation of the rotational velocity in StH α 190: a clear minimum is found at 100 km s^{-1} (the lowest value found for χ^2 is used to normalize the other values). Bottom panel: the critical break-up velocity as a function of stellar mass for various values of stellar surface gravities. The dashed horizontal line with arrows shows $v \sin i$ for StH α 190 (the arrows indicate that this is a lower limit to the true equatorial rotational velocity).

Fig. 3.— Derivations of abundances and stellar parameters are illustrated here. Top panel: abundances of [Fe I/H], [Fe II/H], and [Ba II/H] versus T_{eff} for model atmospheres with $\log g= 3.0$ and microturbulence set to 2.0 km s^{-1} . Note that Fe I and Fe II give the same abundances for $T_{\text{eff}}= 5300\text{K}$, and that [Ba II/H] is always larger than [Fe/H]. Bottom panel: the G-type star in StH α 190 is placed in a $T_{\text{eff}} - \log g$ plane, along with stellar model evolutionary tracks from Schaerer (1993). This comparison indicates that the yellow component of StH α 190 is an intermediate-mass subgiant about to begin its ascent of the red giant branch.

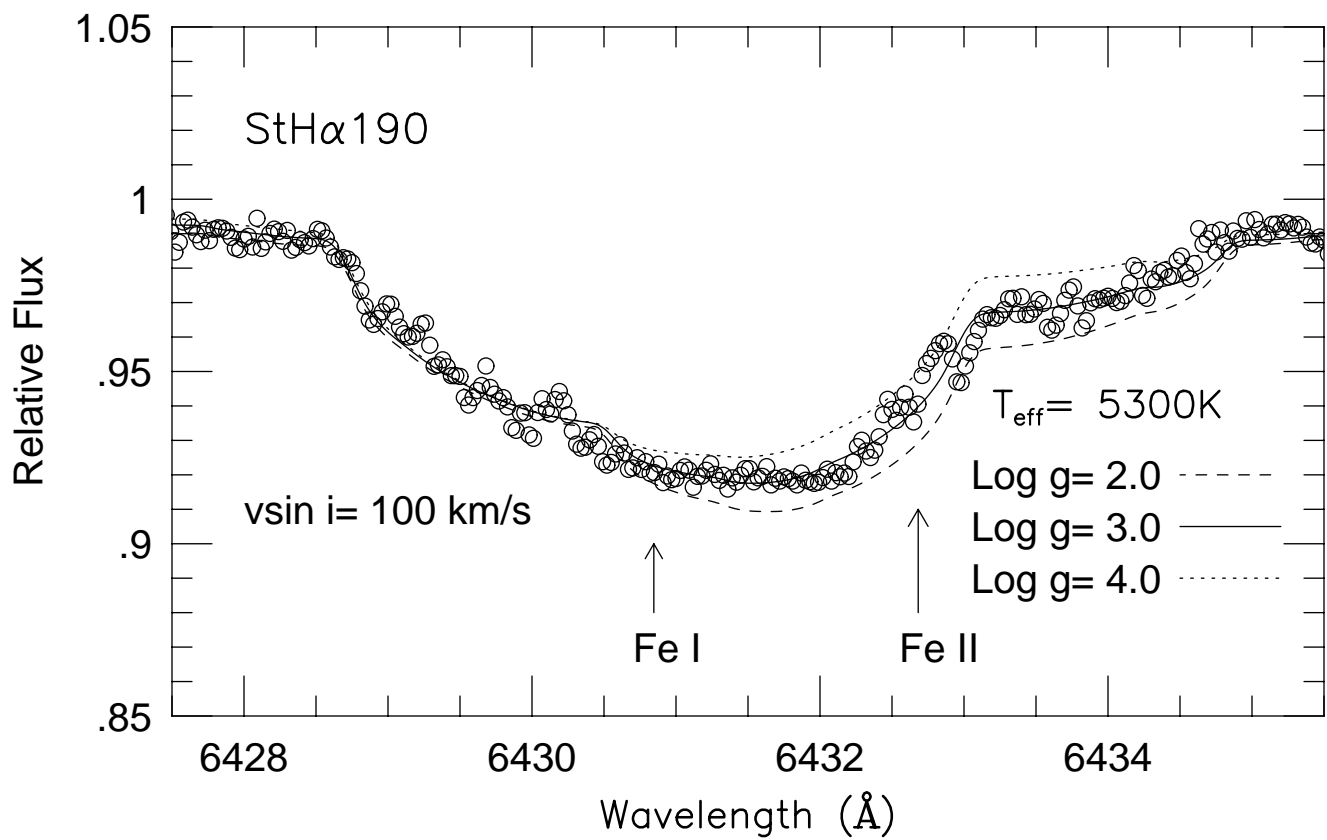
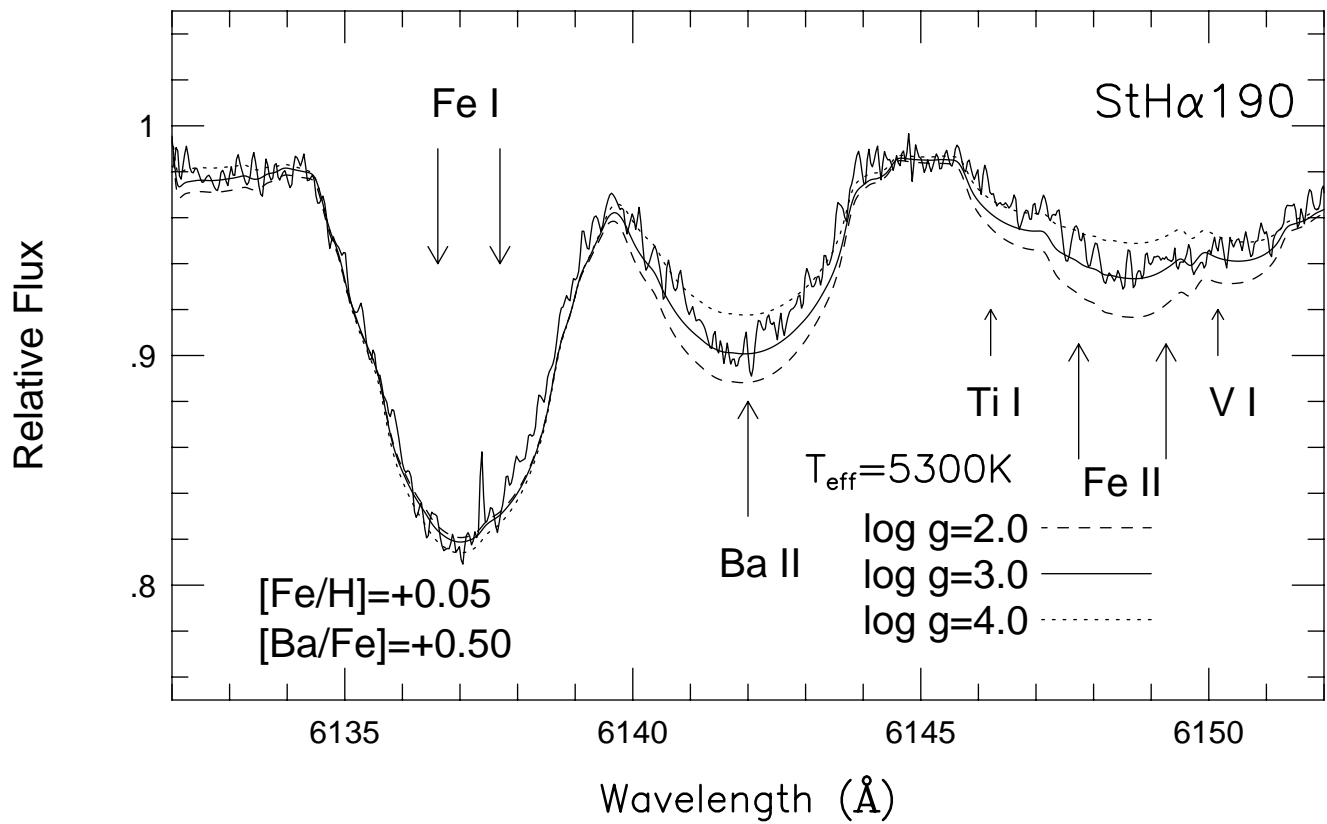


TABLE 1
HELIOCENTRIC RADIAL VELOCITIES

Date	Time (UT)	Integration	V_{rad} (km s ⁻¹)	Observatory
1995 Nov. 29	02:50	60 ^m	+9.8 ± 1.0	McDonald
1996 Jul. 7	07:48	30 ^m	+15.3 ± 1.5	McDonald
1996 Jul. 7	09:15	30 ^m	+13.8 ± 1.5	McDonald
1996 Jul. 8	08:50	20 ^m	+13.7 ± 2.0	McDonald
1999 Oct. 27	01:05	120 ^m	+14.6 ± 1.0	ESO
2001 May 17	09:10	40 ^m	+1.6 ± 2.0	ESO
2001 May 18	09:15	40 ^m	+4.1 ± 1.5	ESO
2001 May 19	07:15	40 ^m	+2.4 ± 1.5	ESO
2001 May 19	09:25	30 ^m	+0.0 ± 2.0	ESO

